Published in final edited form as:
*New J Phys*. 2007 ; 9: 127. doi:10.1088/1367-2630/9/5/127.

# Miniaturized side-viewing imaging probe for fluorescence lifetime imaging (FLIM): validation with fluorescence dyes, tissue structural proteins and tissue specimens

**D S Elson**[1], **J A Jo**[2,3], and **L Marcu**[2]

1 *Institute of Biomedical Engineering and Department of Biosurgery and Surgical Technology, Imperial College London, Exhibition Road, London SW7 2AZ, UK*

2 *Department of Biomedical Engineering, University of California Davis, Genome and Biomedical Sciences Building, 451 East Health Sciences Drive, Davis, CA 95616, USA E-mail: lmarcu@ucdavis.edu*

## Abstract

We report a side viewing fibre-based endoscope that is compatible with intravascular imaging and fluorescence lifetime imaging microscopy (FLIM). The instrument has been validated through testing with fluorescent dyes and collagen and elastin powders using the Laguerre expansion deconvolution technique to calculate the fluorescence lifetimes. The instrument has also been tested on freshly excised unstained animal vascular tissues.

## 1. Introduction

Time-resolved fluorescence spectroscopy is a promising non- or minimally-invasive and non-destructive method that has been demonstrated as a usable discrimination method between different tissue compositions [1]. This method has previously been validated for discriminating atherosclerotic plaques [1], and detection of glioma tissue [2], by investigating the fluorescence spectral-lifetime signatures of isolated prepared tissue components (e.g. collagen and elastin powders and lipids), *ex vivo* tissue specimens of diseased tissues (tumours, atherosclerotic plaques), *in vivo* animal models mimicking diseases [3], and more recently *in vivo* in clinical settings [4]. The work reported here presents the next step in the progression from laboratory to bedside by addressing two further clinical needs: (i) a miniaturized flexible probe that can be used for endoscopic or intravascular diagnostics, and (ii) an image guidance technique for improved navigation, tissue discrimination and quicker clinical assessment. Fluorescence lifetime imaging microscopy (FLIM) is a technique that is able to record large amounts of lifetime information in an image format, and may be combined in a number of ways with emission spectroscopy. The lower spectral-lifetime resolution that results from using an imaging modality with a limited acquisition time is compensated for by selecting the spectral bands that reveal the maximum contrast based on previous single-point spectroscopy experiments. In this paper, we demonstrate a fluorescence spectral-lifetime imaging flexible side-viewing endoscope which is tested on fluorescent dyes, collagen and elastin powders and freshly excised animal cardiovascular tissues.

We have recently shown that the Laguerre polynomial approach to fitting fluorescence lifetime decays is an effective method for deconvolving the instrument response function (IRF), and

Correspondence to: L Marcu.
[3]Current address: Department of Biomedical Engineering, Texas A&M University, 3120 TAMU, TX, USA.

provides a number of advantages over forward convolution and nonlinear least-squares fitting methods of calculating ideal fluorescence decays [5,6]. For instance, the Laguerre polynomials need only be convolved with the recorded IRF once each, before being used in the expansion of the recorded fluorescence decay. This is a linear process and is computationally much less intensive than fitting methods—a property that is especially important in FLIM where a large number of parallel lifetime measurements must be analysed. In addition, the Laguerre functions form a complete and orthogonal basis, allowing a complete and unambiguous expansion of the fluorescence decay, a definite advantage over multiple exponential decay approaches, which often produce ambiguous results due to the presence of noise and the well-known interdependence between the lifetimes and initial intensities [7]. After the expansion is calculated the initial intensity and average fluorescence lifetime can be calculated, with the addition of a basis of Laguerre coefficients for each pixel, which have previously been shown to produce additional useful contrast in biological specimens including atherosclerotic plaque [5]. The FLIM data reported in this paper was analysed using this new approach.

FLIM allows the localization and mapping of fluorophore distributions so that structural, chemical and environmental information may be contrasted across the field of interest. To be able to image temporally resolved fluorescence decays, the most commonplace methods include using time-correlated single photon counting (TCSPC) and single point scanning, or time- or frequency-modulated microchannel plate image intensifiers. Most FLIM systems that have been demonstrated using rigid or flexible endoscopes have used a microchannel plate image intensifier approach due to the faster acquisition times that are achievable in practice, and because they may be more readily coupled to existing medical imaging devices such as endoscopes and arthroscopes (although these devices may require some engineering to accept laser excitation and to lower the temporal dispersion of the light during transmission). We have used a gated microchannel plate image intensifier in this study that is coupled to a flexible fibre image bundle.

There are a number or alternative methods of performing emission wavelength resolved fluorescence lifetime imaging using a GOI as the detector. When only a few, fixed emission wavelength bands are of interest, a dichroic based image splitting device is an attractive option. In this case multiple spectrally resolved images of the sample are arranged on a single detector and image registration methods are used to extract the spectral information pixel by pixel [8]. A more flexible approach with a higher possible spectral resolution is to use an imaging spectrograph to record $x{-}\lambda$ images of a line on the sample, and then to scan the sample in the $y$-direction [9]. Depending on the detector used, this approach may come at the expense of lower signal per pixel, and therefore a lower signal-to-noise, and also a lower acquisition speed due to the requirement of line scanning the sample (one image must be recorded for every $y$ line in the final image). For flexibility and also to maximize the recorded signal, we have chosen to use a filter wheel in the emission path of the instrument so that the emission bands can be chosen depending on the sample, as explained in the method section.

Although single point endoscopic probes for recording lifetime and/or emission resolved spectroscopy are being widely applied [3,10], there have been relatively few reports of FLIM applied through endoscope systems. A frequency-domain endoscopic FLIM instrument for video-rate FLIM of biological tissue was reported with a spatial resolution of 32 × 32 pixels, recording phase resolved images and assuming a mono-exponential decay [11]. In the time domain, two wide-field endoscopic FLIM systems have been demonstrated, one using a flexible fibre bundle endoscope [12], and another one using a rigid arthroscope system [13]. This study aims (i) to develop a FLIM apparatus using a side-viewing flexible fibre bundle probe that may be made compatible with intravascular catheters and flexible endoscopic probes; (ii) to apply the more robust and computationally fast Laguerre polynomial approach [5] to fitting FLIM data collected with the flexible probe, and (iii) to determine whether the

spectral lifetime signature of tissues specimens that have been previously observed with single point spectroscopy can be retrieved from FLIM data. In addition, the validation of this apparatus was conducted on freshly excised cardiovascular tissue specimens. This approach allows for testing the compatibility of FLIM apparatus with imaging of cardiovascular diseases (i.e. atherosclerosis), a major area of research in our laboratory.

## 2. FLIM probe set-up

Flexible optical endoscopes utilize coherent fibre bundles (fibre image guides) to relay the image from the sample to the detector. Although these results in loss of image quality and intensity compared to rigid rod lens endoscopes, rigid systems cannot be applied to intravascular imaging or endoscopic evaluations that require flexible endoscopes. To increase the signal over previous [12] FLIM fibre bundle systems, we have reduced the number of resolution elements to 10 000 coherent fibres (Sumitomo Electric USA, Inc.), and reduced the field-of-view (FOV) and working distance (WD) design parameters (simultaneously increasing the fluorescence signal and providing compatibility with intravascular use). Two fibre bundle endoscopes with a diameter of 0.6 mm were used for this work, both of which had a graded index (GRIN) objective lens with a diameter of 0.5 mm, and an NA (numerical aperture) of 0.5 cemented on to one end of the fibre bundle (Grintech GmbH). One bundle was 0.9 m long and was forward-viewing. A second 2 m long bundle was made to be side-viewing by cementing a BK7 90 degree 0.5 mm edge length polar prism (Grintech GmbH) on to the GRIN lens, for intravascular compatibility (see figure 1). The proximal ends of the endoscopes were cut and polished, and both endoscopes had an image area of 4 mm diameter with a working distance of 4 mm. Factors affecting throughput of the system include the collection NA, fibre core fill factor and fibre attenuation, which are 0.13, 36% and 0.2 dB $m^{-1}$ respectively.

The fluorescence emitted from the proximal end of the fibre bundle was imaged onto the GOI with a × 10 or × 20 microscope objective and a 15 cm focal length doublet lens, which acted like a tube lens in an infinity corrected microscope system. This configuration allowed the insertion of filters into the infinity space without the introduction of spherical aberrations. The filters were held in an electronically changeable filter wheel so that FLIM series at multiple fluorescence wavelengths could be recorded. Three bandpass filters were used throughout this study (central wavelength/bandwidth): 390/70, 450/65 and 550/100 nm.

The fluorescence was excited with a nitrogen laser (337 nm, 700 ps, 20 Hz, LTB Lasertechnik Berlin GmbH) coupled to a separate high numerical aperture (0.4) 200 $\mu$m core diameter polymer fibre (Thorlabs Inc.). The bare distal end of the fibre was positioned to give a spot diameter of 6 mm overlapping with the image field from the fibre endoscope. The typical pulse energy at the sample was 10–20 $\mu$J, which resulted in an exposure of 0.5 $\mu$J $mm^{-2}$. A series of up to 38 time-gated images were recorded on the GOI system (Picostar, LaVision GmbH) with a 1 ns gate width, 500 ps gate separation and 1 or 2 s CCD (charge coupled device) integrations.

The images were subsequently analysed using the Laguerre polynomial deconvolution technique to calculate the fluorescence lifetime, integrated intensity and Laguerre coefficients [5,6]. Briefly, the Laguerre functions (LEC-0, LEC-1, etc) contain a built-in exponential term that results in a convenient expansion of exponential decays, while also forming a complete orthogonal set that allows a fast and complete expansion. After the Laguerre functions have been convolved with the IRF the Laguerre coefficients may be estimated by least squares fitting of a composite Laguerre function to the recorded fluorescence decay. The parameter $\alpha$ that is found in the Laguerre polynomials was fixed at 0.88 based on the Kernel memory length and the number of Laguerre functions, so that the functions decay sufficiently close to zero by the end of the decay [6]. Usually the first four Laguerre functions are sufficient to recreate the fluorescence decay, and the resulting function can then be used to calculate the average

fluorescence lifetime (by computing the interpolated time at which the intensity falls to 1/*e* of the initial intensity) and integrated intensity of the data. Alternatively, the Laguerre expansion coefficients (LEC-0, LEC-1, etc) can themselves be used as additional contrast parameters for the discrimination of different tissue types. Our initial results showed that the Laguerre deconvolution method was able to retrieve the lifetime maps correctly and extremely fast without *a priori* assumptions of the decay shape of the fluorescence. As previously demonstrated, this technique also enabled rapid processing of data and access to contrast parameters consisting of the Laguerre coefficients. Tissue FLIM images presented in this paper took less than 1.5 s for 260 × 344 pixels using an algorithm that has been implemented in Matlab that is run in a PC with a 2.66 GHz Intel Core 2 Duo processor.

## 3. FLIM system validation: methods and results

### 3.1. Temporal and spectral response

The instrument was tested on a series of three different fluorescent dyes (DPS, Coumarin 440 and Stilbene 420 dissolved in ethanol) to validate the temporal and spectral response. The lifetime values at each pixel have been calculated based on the Laguerre expansion technique described above, and an average lifetime was computed by averaging the resulting lifetime map. Processing time for these 480 × 608 pixel images was less than 4 s. Comparisons with the values reported in the broad literature are difficult due to the dependence of the solvent and emission wavelength on the fluorescence lifetime recorded. Nevertheless, our values are consistent with results published previously [14]–[16]. We have also compared the average fluorescence lifetimes retrieved with the current FLIM system with those found using the previously reported single-point time-resolved laser-induced fluorescence system (TR-LIFS) [5,17] (table 1). This instrument has a higher 300 ps temporal resolution and has been tested on dye solutions and fluorescence lifetime standards [17].

It can be seen that the lifetimes agree well between the two systems, and the variations between the two systems and across the emission spectrum are attributed to the deconvolution process. Representative fluorescence lifetime maps for the three dye solutions recorded through the forward-viewing endoscope are presented in figure 2. Figure 2 also depicts the reconstructed fluorescence decay at a sample pixel of the FLIM image from Coumarin 440 together with the estimated decay after deconvolution and the corresponding estimation error. The low level of the estimation error and its autocorrelation function shown below indicate the excellent performance of the deconvolution method.

In addition, the FLIM system was tested on dry powder samples of collagen type II from bovine Achilles tendon (Sigma-Aldrich) and elastin from bovine neck ligament (Sigma-Aldrich). The results are summarized in table 1 and figure 2. The collagen and elastin fluorescence properties agree with those previously reported [17]. Collagen shows higher intensity at the 390 nm band, while elastin shows stronger fluorescence at the 450 nm band. There is a trend towards lower lifetimes as the emission wavelength band increases in both substances, although this was most pronounced for collagen (figure 2).

### 3.2. Spatial resolution

The spatial resolution of the endoscope was also tested by using a USAF test chart, which fluoresced under the UV excitation (Edmund Optics pocket USAF target). At a WD of 4 mm the forward viewing endoscope was able to resolve group 2, element 6, and the side-viewing endoscope was able to resolve group 3 element 2. These correspond to 7.13 and 8.98 line pairs per millimetre respectively, or a feature size of 70 and 56 $\mu$m.

### 3.3. Validation on tissue specimens

FLIM maps were recorded from freshly excised cardiovascular tissues including rat aortic, and pig coronary and aortic arteries. Figure 3 shows a fluorescence data set from a sample of rat aorta lumen (intensity maps, lifetime maps and Laguerre coefficient LEC-1 maps representative of the contrast available from the Laguerre coefficients, at three different emission bands). Prior to experiments, the aorta was washed in saline buffer, dissected longitudinally and placed flat on a dark rubber with the lumen facing up. The fluorescence intensity was strong with both the 390 and 450 nm bandpass filters, reflecting the presence of both elastin (from media) and collagen (from adventitia), as was confirmed by histopathology. The lifetime maps also indicate a combination of both elastin and collagen. The presence of a brighter spot with shorter lifetime values with the 450 nm bandpass filter (indicated by the red arrows), suggests a stronger elastin component. This could be due to a thickening of the elastin rich intima at that specific location, although histopathological confirmation was not performed at this site.

The ability of the instrument to reveal structural contrast was not realized when imaging the lumen since there is no structure in normal arterial intima. Instead, we have imaged the different layers of artery cross-sections to demonstrate the ability of the endoscopic system to distinguish different tissue types and composition. A pig coronary cross-section was imaged and contrast was observed between low fluorescence myocardium and highly fluorescence elastin rich arterial wall, mainly from the media. Results are presented in figure 4, together with the cross-section picture and a histopathology slice taken from the same sample. The white-light picture does not show clear demarcation between arterial wall and surrounding myocardium tissue. Histology shows an elastin-rich media. The fluorescence intensity is higher and the lifetime is shorter for the 450 nm bandpass filter, reflecting the elastin component. The Laguerre coefficient LEC-1 also provides high contrast between the arterial wall and the myocardium tissue. A summary of the fluorescence lifetimes found for the various tissue samples (including the ones shown in figures 3 and 4) is presented in table 2, showing the peak fluorescence emission band and the mean lifetimes for the three emission bands.

## 4. Conclusions

We have demonstrated an instrument for fluorescence lifetime imaging in a flexible side-viewing endoscope that is compatible with intravascular imaging constraints. This constrained environment required a short WD and high NA GRIN objective, which should result in a higher photon collection efficiency over the only previously reported flexible endoscope [12]. The other FLIM endoscopes published in the literature are rigid rod lens devices operating in the frequency domain [11] and the time-domain [13] which are unsuitable for intravascular use. The performance of the flexible imaging probe has been validated using fluorescent lifetime dyes and samples of elastin and collagen (the main fluorescent constituents in arteries and other tissues). These values were compared with results recorded with our time-resolved single-point spectrometer and values from the literature.

Finally, the instrument was applied to imaging of freshly excised animal cardiovascular tissues, showing the ability to distinguish between elastin rich and collagen rich tissues. While the system is able to accurately record spectrally resolved fluorescence lifetimes, the time taken to acquire all of the data is currently too long for clinical application, where movements are expected to lead to lifetime artefacts. In future, the acquisition speed will be increased through further reference to the single point spectroscopy system so that the optimum number of gates, gate separation and spectral pass-bands can be chosen. Applications of this instrument concern diagnosis of human diseases including intravascular diagnosis of high-risk atherosclerotic plaques.

## Acknowledgments

This work was supported in part by the National Institute of Health grant R01 HL 67377. We also acknowledge support from the National Science Foundation Centre for Biophotonics Science and Technology at University of California Davis and the continued help and assistance of Dr Christopher Hollars. We are grateful to Professor Martin Gundersen of University of Southern California for providing the gated imaging camera used in this study. During the period of the study, Dr Daniel Elson was a visiting scholar at the Department of Biomedical Engineering, UC Davis.

## References

1. Marcu L, Fishbein MC, Maarek JM, Grundfest WS. Discrimination of human coronary artery atherosclerotic lipid-rich lesions by time-resolved laser-induced fluorescence spectroscopy. Arterioscler Thromb Vasc Biol 2001;21:1244–50. [PubMed: 11451759]
2. Yong WH, Butte PV, Pikul BK, Jo JA, Fang QY, Papaioannou T, Black KL, Marcu L. Distinction of brain tissue, low grade and high grade glioma with time-resolved fluorescence spectroscopy. Front Biosci 2006;11:1255–63. [PubMed: 16368511]
3. Marcu L, Fang QY, Jo JA, Papaioannou T, Dorafshar A, Reil T, Qiao JH, Baker JD, Freischlag JA, Fishbein MC. *In vivo* detection of macrophages in a rabbit atherosclerotic model by time-resolved laser-induced fluorescence spectroscopy. Atherosclerosis 2005;181:295–303. [PubMed: 16039283]
4. Marcu, L.; Jo, JA.; Fang, Q.; Papaioannou, T. Applications of time-resolved fluorescence spectroscopy to atherosclerotic cardiovascular disease and brain tumours diagnosis. Conf. on Lasers and Electro-Optics (CLEO); Baltimore, Optical Society of America. 2005.
5. Jo JA, Fang QY, Papaioannou T, Marcu L. Fast model-free deconvolution of fluorescence decay for analysis of biological systems. J Biomed Opt 2004;9:743–52. [PubMed: 15250761]
6. Jo JA, Fang QY, Marcu L. Ultrafast method for the analysis of fluorescence lifetime imaging microscopy data based on the Laguerre expansion technique. IEEE J Sel Top Quantum Electron 2005;11:835–45.
7. Grinwald A. On the analysis of fluorescence decay kinetics by the method of least-squares. Anal Biochem 1974;59:583–93. [PubMed: 4838786]
8. Siegel J, et al. Whole-field five-dimensional fluorescence microscopy combining lifetime and spectral resolution with optical sectioning. Opt Lett 2001;26:1338–40. [PubMed: 18049601]
9. Schultz RA, Nielsen T, Zavaleta JR, Ruch R, Wyatt R, Garner HR. Hyperspectral imaging: a novel approach for microscopic analysis. Cytometry 2001;43:239–47. [PubMed: 11260591]
10. Pfefer TJ, Paithankar DY, Poneros JM, Schomacker KT, Nishioka NS. Temporally and spectrally resolved fluorescence spectroscopy for the detection of high grade dysplasia in Barrett's esophagus. Lasers Surg Med 2003;32:10–6. [PubMed: 12516065]
11. Mizeret J, Wagnieres G, Stepinac T, van Den Bergh H. Endoscopic tissue characterization by frequency-domain fluorescence lifetime imaging (FD-FLIM). Lasers Med Sci 1997;12:209–17.
12. Siegel J, et al. Studying biological tissue with fluorescence lifetime imaging: microscopy, endoscopy, and complex decay profiles. Appl Opt 2003;42:2995–3004. [PubMed: 12790450]
13. Requejo-Isidro J, et al. High-speed wide-field time-gated endoscopic fluorescence lifetime imaging. Opt Lett 2004;29:2249–51. [PubMed: 15524370]
14. Koti ASR, Periasamy N. Solvent exchange in excited-state relaxation in mixed solvents. J Fluorescence 2000;10:177–84.
15. Munro I, et al. Towards the clinical application of time-domain fluorescence lifetime imaging. J Biomed Opt 2005;10:051403. [PubMed: 16292940]
16. Tan X, Gustafson TL. Solvent-solute interactions probed by picosecond time-resolved fluorescence spectroscopy: lifetime and anisotropy study of S-1 trans-4,4′-diphenylstilbene. J Phys Chem A 2000;104:4469–74.
17. Fang QY, Papaioannou T, Jo JA, Vaitha R, Shastry K, Marcu L. Time-domain laser-induced fluorescence spectroscopy apparatus for clinical diagnostics. Rev Sci Instrum 2004;75:151–62.

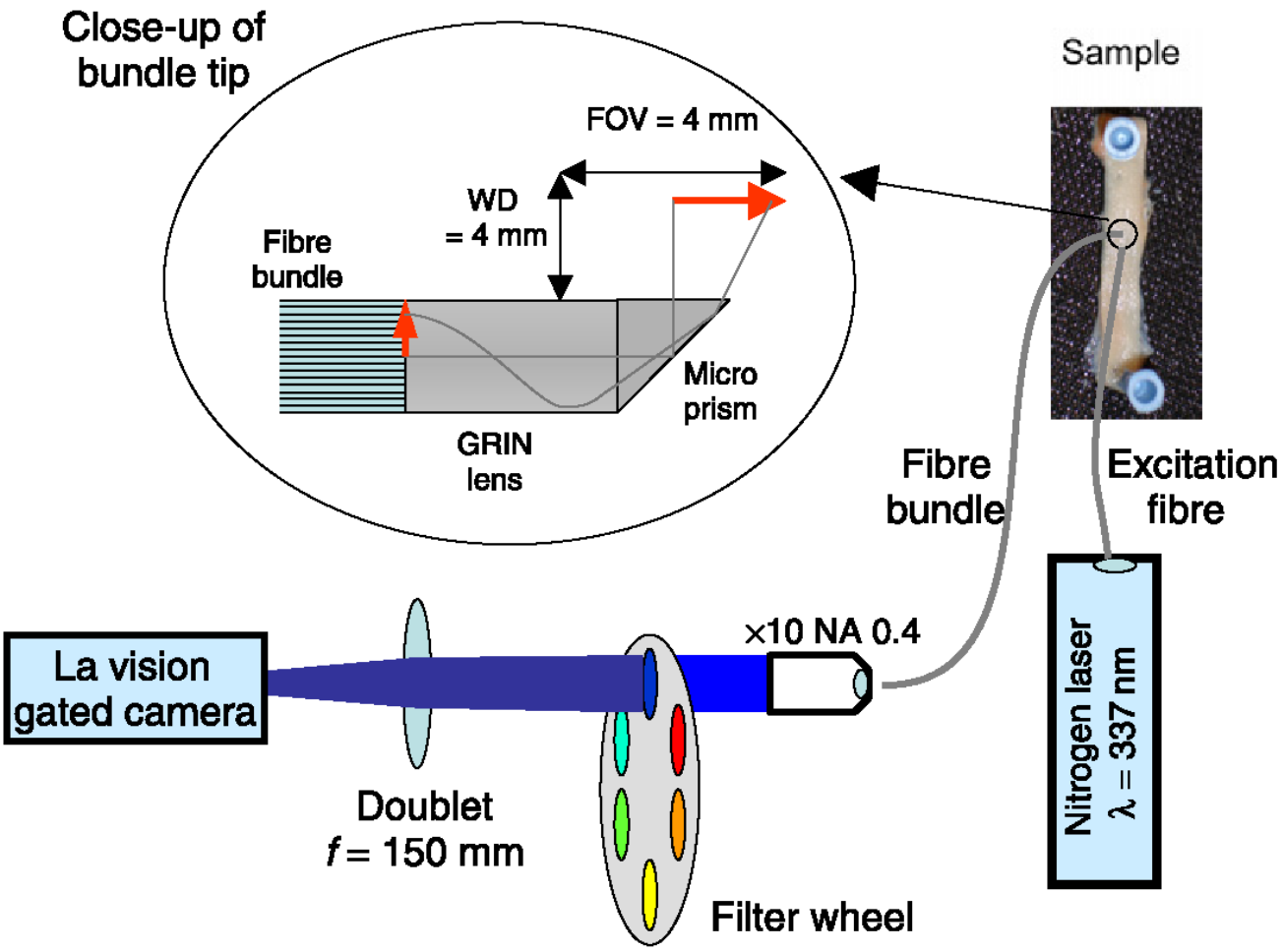


**Figure 1.**
Schematic of the FLIM experimental set-up to transmit the 4 mm FOV at 4 mm WD through the fibre bundle and onto the gated camera.

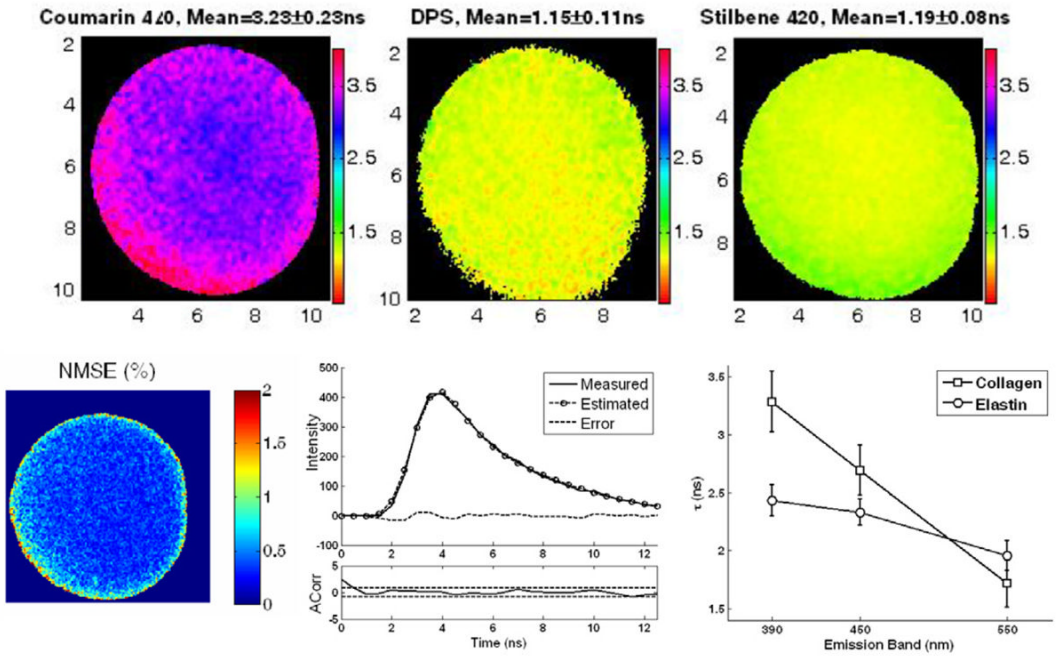


**Figure 2.**

Top: lifetime maps from the three different dye solutions Coumarin 440, DPS and Stilbene 420 (dissolved in ethanol) obtained with the 450, 390 and 450 nm bandpass filters, respectively. Bottom left: plot of normalized mean square error (NMSE) at every pixel, showing that it is less than 2% across the FOV. Bottom centre: a representative single pixel decay from Coumarin, together with the estimated fluorescence decay and autocorrelation. Bottom right: average lifetime obtained from the FLIM analysis of collagen and elastin with the 390 nm, 450 nm and 550 nm bandpass filters.

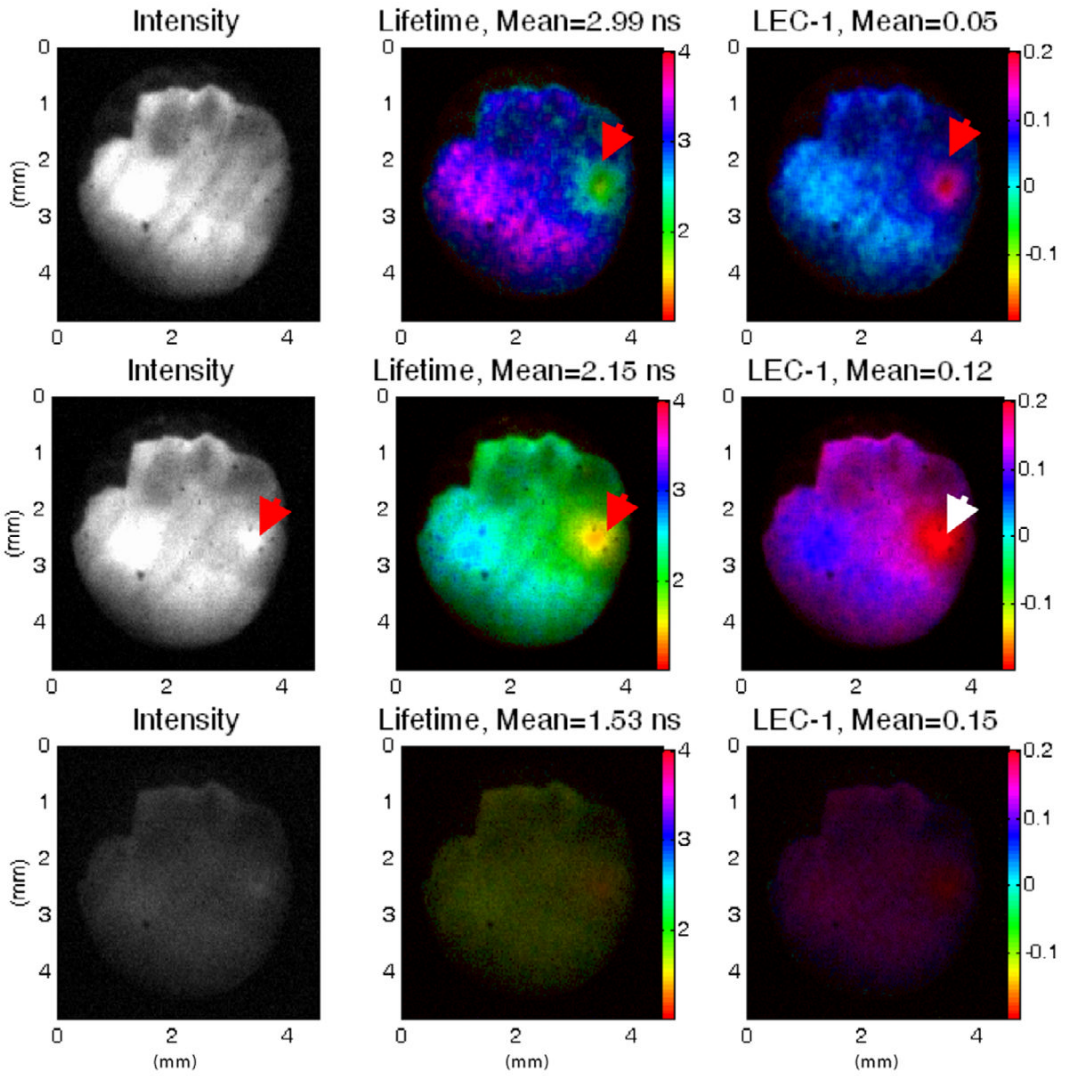


**Figure 3.**

FLIM images of rat aorta lumen showing the intensity (left), lifetime (middle) and Laguerre coefficient LEC-1 (right) maps, measured with the 390 nm (top), 450 nm (middle) and 550 nm (bottom) bandpass filters. The arrows indicate an area rich in elastin, which cannot be seen from the intensity maps at 390 nm but can be clearly detected in the lifetime and LEC-1 maps at that emission band. With the 450 nm emission band, the elastin-rich spot can also be clearly observed in the intensity map.

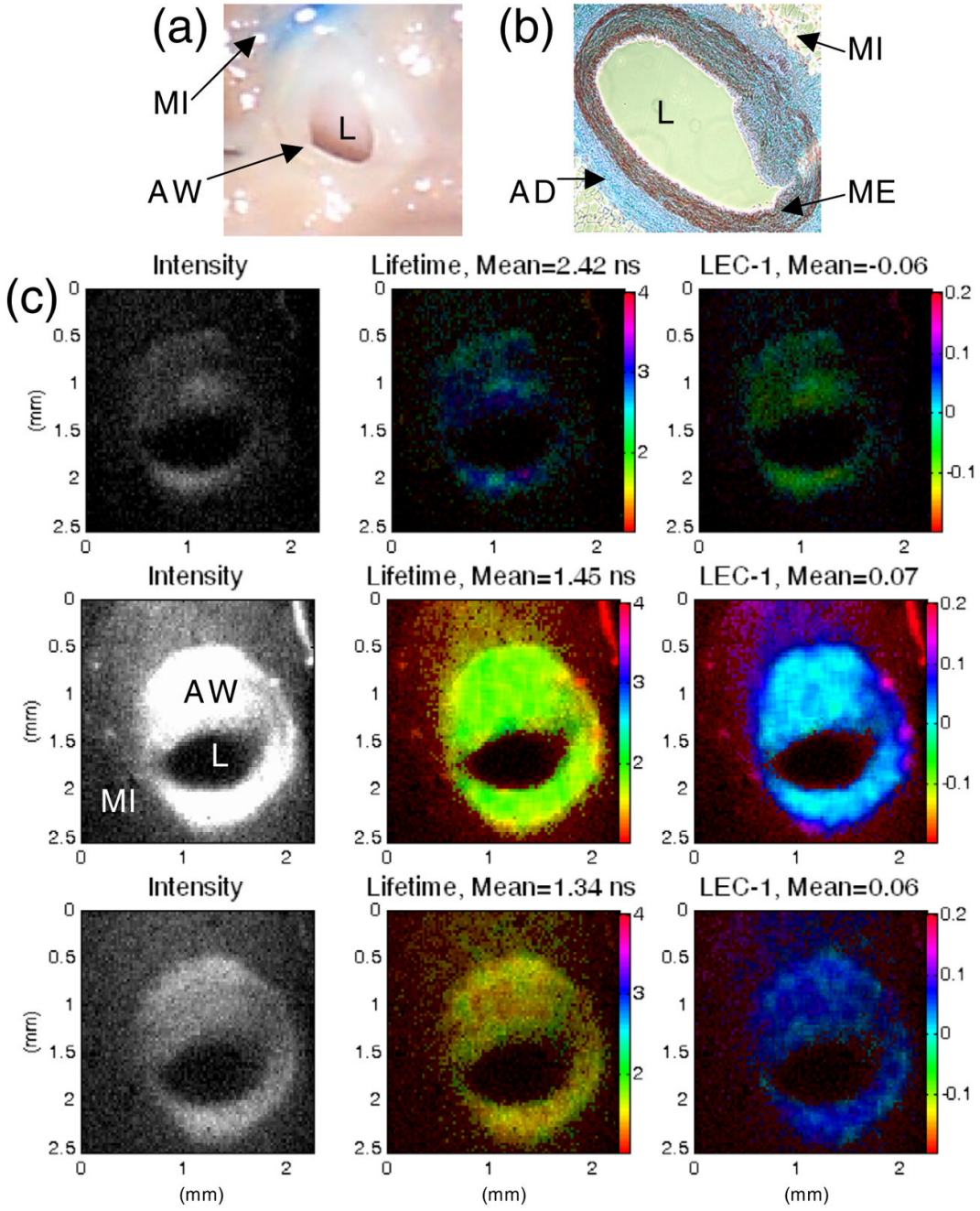


**Figure 4.**

(a) Photograph of the cross-section of the pig coronary artery, showing the arterial wall (AW), lumen (L), and surrounding myocardium tissue (MI). (b) Histology section showing the elastin rich media (ME) and collagen rich adventitia (AD) of the arterial wall. (c) FLIM images showing the intensity (left), lifetime (middle) and Laguerre coefficient LEC-1 (right) maps, measured with the 390 nm (top), 450 nm (middle) and 550 nm (bottom) bandpass filters. While the photograph does not show clear demarcation between AW and surrounding MI, the fluorescence intensity and lifetime maps shows contrast between the two tissue types. The intensities are higher and lifetimes are shorter at 450 nm, reflecting a strong elastin component

in the AW. LEC-1 also shows high contrast between the coronary cross-section and surrounding tissues.

**Table 1**

Validation of flexible FLIM probe compared with TR-LIFS for various test dyes and collagen and elastin powders.

| | Peak emission band (nm) | Lifetimes (ns) | | | |
|---|---|---|---|---|---|
| | | FLIM | | | |
| | | 390 nm | 450 nm | 500 nm | TR-LIFS |
| Coumarin 440 | 450 | 3.26 | 3.27 | 3.29 | 3.29 (450 nm) |
| DPS | 390 | 0.98 | 0.92 | 0.85 | 1.09 (390 nm) |
| Stilbene 420 | 390/450 | 1.03 | 0.97 | 0.92 | 0.89 (450 nm) |
| | | 390 nm | 450 nm | 550 nm | |
| Collagen | 390 | 3.26 | 2.66 | 1.69 | |
| Elastin | 450 | 2.41 | 2.32 | 1.95 | |

*New J Phys*. Author manuscript; available in PMC 2009 June 5.

**Table 2**

Summary of the mean lifetimes calculated for tissue.

| | Peak emission band (nm) | Mean lifetimes (ns) | | |
|---|---|---|---|---|
| | | 390 nm | 450 nm | 550 nm |
| Rat aorta lumen | 390/450 | 2.99 | 2.15 | 1.53 |
| Rat aorta adventitia | 390/450 | 3.40 | 2.36 | 1.64 |
| Rat aorta cross-section | 450 | 2.69 | 2.09 | 1.72 |
| Pig coronary cross-section | 450 | 2.42 | 1.45 | 1.34 |
| Pig aorta cross-section | 450 | 2.86 | 2.84 | 2.05 |